Multi-response kinetic modelling of the formation of five Strecker aldehydes during kilning of barley malt

José A. Piornos, Dimitris P Balagiannis, Elisabeth Koussissi, August Bekkers, Johan Vissenaekens, Eric Brouwer, Jane K Parker

HAL Id: hal-04791657

https://hal.inrae.fr/hal-04791657v1

Submitted on 19 Nov 2024

Contents lists available at ScienceDirect

Food Chemistry

Multi-response kinetic modelling of the formation of five Strecker aldehydes during kilning of barley malt

José A. Piornos [a,1], Dimitris P. Balagiannis [a,*], Elisabeth Koussissi [b,2], August Bekkers [b], Johan Vissenaekens [c], Eric Brouwer [b], Jane K. Parker [a]

[a] *Department of Food and Nutritional Sciences, University of Reading, RG6 6DZ, UK.*
[b] *Heineken Supply Chain BV, Global Innovation & Research, Burgemeester Smeetsweg, 1, 2382, PH, Zoeterwoude, the Netherlands.*
[c] *Mouterij Albert, Kanaaldijk, 2870 Ruisbroek-Sint-Amands, Belgium.*

ARTICLE INFO

ABSTRACT

Control of aroma formation during production of barley malt is critical to provide consistent and high-quality products for the brewing industry. Malt quality can be affected by the inherent variability of raw material and processing conditions, leading to inconsistent and/or undesirable profiles. Dried green malts were cured isothermally at 65, 78 and 90 °C for 8.4 h, and characteristic aroma compounds (Strecker aldehydes), precursors and intermediate compounds were analysed over time. By kinetic modelling of Strecker aldehydes, based on fundamental chemical pathways, we showed that degradation of Amadori rearrangement products and short-chain dicarbonyls was more sensitive to temperature change due to their higher activation energies compared to other kinetic steps. This study can help maltsters to manipulate formation of Strecker aldehydes, via raw material screening and process control, and hence optimise the organoleptic quality of malts and their products, such as non-alcoholic beers, where these aldehydes play a key role.

1. Introduction

Barley (*Hordeum vulgare* L.) is the fourth most important cereal crop in the world, after wheat, corn and rice. Of the 148 million tons produced worldwide per year (on average between 2014 and 2023 US Foreign Agricultural Service, 2024), 27 % is used for the production of barley malt for use by the brewing industry (Akar et al., 2004). The malting process consists of three steps: (1) steeping to hydrate the seed kernels from around 12 % to at least 40 % moisture; (2) germination to activate the production of hydrolytic enzymes (proteases, amylases and

others) and cell wall breakdown; and (3) kilning, initially to dry the kernels at low temperature (drying step), and then to generate flavour compounds and colour at higher temperatures (curing step) (Gupta et al., 2010). During the curing step, the volatile compounds that give malt its characteristic aroma are formed. A range of volatile compounds have been identified as responsible for the characteristic aroma of this cereal product (Beal & Mottram, 1994).

Strecker aldehydes are formed via the Strecker degradation of free amino acids when they react with Maillard reaction derived α-dicarbonyl compounds (Rizzi, 2008). In particular, germination of the barley grains generates a blend of amino acids and reducing sugars from the degradation of proteins and starches, respectively (Huang et al., 2016; Steiner et al., 2011; Zhang & Jones, 1995). During the Maillard reaction, a series of consecutive and simultaneous reactions produce some intermediate compounds, such as Amadori reaction products (ARP) or the highly reactive short chain dicarbonyls (SCDC) (Meitinger et al., 2014; Smuda & Glomb, 2013). These SCDC, in turn, can react with amino acids, finally forming aldehydes during the Strecker degradation (Balagiannis et al., 2009). The nature of the Strecker aldehyde formed depends on the amino acid of origin. For instance, methionine, valine, isoleucine, leucine, and phenylalanine produce methional (potato-like aroma), 2-methylpropanal (malty), 2-methylbutanal (malty), 3-methylbutanal (malty), and phenylacetaldehyde (honey), respectively.

The distinct aroma of the different types of malts is developed during kilning and it is strongly dependent on both processing conditions (e.g., time and temperature) and raw materials (e.g., precursors concentration, moisture content) which are subjected to the inherent variability of a living system. Gu et al. (2022) showed that barley malts kilned at increasing temperatures contained higher concentrations of 3-methylbutanal and phenylacetaldehyde. The effect of these variables has been studied using mathematical models in order to better understand their role in the final product. An empirical mathematical model (based on response surface methodology) for the formation of methional and phenylacetaldehyde in Australian barley malt showed that the concentration of those compounds increased with kilning time and temperature (Huang, Yu, et al., 2016). Unlike empirical models, mechanistic models take into account the behaviour of both the precursors and the products, as well as intermediate compounds. For this purpose, multi-response kinetic modelling has been used to generate, analyse and evaluate mechanistic models (Balagiannis, 2015). Huang, Tippmann, and Becker (2016) proposed a kinetic model for the formation of 2- and 3-methylbutanal from sugar (glucose or maltose) and amino acid (leucine or isoleucine) in a phosphate buffer medium, a simplified model system simulating the wort boiling conditions. They proposed a formation mechanism based on two consecutive reactions where each sugar reacts with each amino acid to produce an intermediate, and this forms the corresponding Strecker aldehyde. Other kinetic models for the formation of these aldehydes have been developed in more complex real food matrices (Balagiannis et al., 2009).

In the case of Strecker aldehydes, quantitative control of their formation during kilning is critical because, even though appreciated in malts, these compounds are responsible for the malty and worty off-notes of some malt-derived products, such as alcohol-free beers (Perpète & Collin, 2000; Piornos et al., 2020). In these beers, Strecker aldehydes, such as methional, 3-methylbutanal and phenylacetaldehyde, are among the main contributors to their aroma (Piornos et al., 2020). Therefore, understanding how the different parameters involved affect their formation is of great importance to be able to manipulate the process and control their levels in malt, and potentially in beer. Thus, the hypotheses of the present research were that (1) the formation of Strecker aldehydes during malt kilning was dependent on the processing conditions (temperature and time) and (2) this takes place via the degradation of relatively reactive sugars (glucose and fructose) and amino acids, with the formation of several intermediates of different stability and reactivity (such as ARP and SCDC). Therefore, the aim of this study was to develop a mechanistic kinetic model, using the

multi-response approach, for the formation of five Strecker aldehydes (2-methylpropanal, 2- and 3-methylbutanal, phenylacetaldehyde and methional) in barley malt during the curing stage of kilning at pilot-scale. A range of temperatures and curing times relative to those used for Lager malts were employed and key kinetic parameters (rate constants and activation energies) were estimated to assess and compare the different kinetic steps that comprise the model. This provides the opportunity for the first time to understand and manipulate the formation of these volatiles in barley malt under industrial-like conditions.

2. Materials and methods

2.1. Preparation of malt samples: micro-malting

Barley was received at Mouterij Albert (Ruisbroek-Sint-Amands, Belgium), steeped in water for one day and germinated for five days at industrial scale. Two different varieties of barley were used in this study: the two-row spring variety 'RGT Planet' and six-row winter variety 'Etincel'. The germinated grains, i.e., the green malt, were kilned using pilot-scale micro-malting equipment from Nordon & Cie. (Nancy, France). Moisture of the green malt samples was measured before the kilning process (Supplementary Table S1). The green malt was placed in cubic shape stainless-steel baskets (150 mm side), split diagonally into two parts by a piece of steel (650 ± 2 g in each side). The micro-malting equipment was provided with eight baskets with grilled bottom to allow hot air to circulate throughout.

The kilning programmes had an initial drying process, starting at 25 °C and reaching 55 °C in 10 min, then increasing to 64 °C in 45 min, kept constant for 4 h and 50 min and raised to 65 °C in 3.25 h. After the drying process, the temperature was increased to the curing temperature (65 °C, 78 °C or 90 °C) in 10 min and kept constant for 8.4 h. Sampling was done only during the curing stage, since no formation of aroma compounds was observed during the drying stage. The baskets were taken out randomly from the different positions in the oven and the empty space replaced by an empty basket with a lid. The total duration of the malting experiments was 16 h and 52 min, and the samples were taken every 72 min only during the curing stage. After kilning, the rootlets were removed by manual rubbing, separated by sieving through a 1.8 × 23 mm mesh and stored in a freezer at −30 ± 1 °C to limit thermal reactions. The kilning experiments were performed in duplicate from two different batches of barley for each variety in different days, except for the experiments at 65 °C, where the duplicates were from the same batch due to availability at the industry on the day of collection.

2.2. Chemicals

2-Methylpropanal (≥ 98 %), 2-methylbutanal (≥ 95 %), 3-methylbutanal (≥ 97 %), methional (≥ 97 %), phenylacetaldehyde (≥ 95 %), 2-methylbenzaldehyde (97 %), a standard of 18 L-amino acids and DL-norvaline (≥ 98 %) were purchased from Sigma-Aldrich (Gillingham, UK). D(+)-glucose anhydrous (99.5 %) and D(−)-fructose (≥ 99 %) were from Fluka (Loughborough, UK) and 2-methylpentanal (≥ 95 %) and D(+)-trehalose dihydrate (≥ 98 %) from TCI (Oxford, UK). LC/MS grade formic acid (≥ 99 %) and ammonium formate were from Fisher Scientific (Loughborough, UK). Acetonitrile (≥ 99 %, LC/MS grade) was supplied by VWR (Lutterworth, UK). N-fructosyl valine (FruVal, CAS no. 10003–64-2, 95 %), N-fructosyl leucine (FruLeu, 34,393–18-5, 95 %), N-fructosyl isoleucine (FruIle, 87,304–79-8, 96 %), N-fructosyl phenylalanine (FruPhe, 31,105–03-0, 95 %), N-fructosyl alanine (FruAla, 16,124–24-6, 95 %), N-fructosyl glycine (FruGly, 60,644–20-4, 95 %), N-fructosyl proline (FruPro, 29,118–61-2, 97 %) were acquired from Toronto Research Chemicals (Toronto, ON, Canada).

2.3. Extraction and quantification of non-volatile compounds

The malt samples were ground using a mill provided with a size 40

mesh. The ground samples (1.0 g) were extracted using 10 mL of ultrapure water (18.2 MΩ) containing 1.25 mM of L-norvaline and 15 μM of trehalose as internal standards for amino acids and sugars, respectively. The samples were stirred for 15 min at approximately 1700 rpm using a MultiReax shaker from Heidolph (Schwabach, Germany). After centrifugation at 5500 ×*g* for 15 min at 4 °C, the aqueous layer was separated, and the pellet was reextracted twice (5 mL × 2). The three extracts were combined and stored at −18 °C until analysis. The extractions were performed in duplicate.

2.3.1. Quantification of free amino acids

For each malt extract, an aliquot (250 μL) was diluted with 1000 μL acetonitrile, centrifuged at 500 ×*g* for 3 min, and filtered through a 0.2-μm syringe filter. The samples (5 μL) were injected in a 1260 Infinity HPLC coupled to a 6410 Triple Quad LC/MS detector, all from Agilent Technologies (Santa Clara, CA, USA). A Synchronis™ HILIC column (150 × 4.6 mm i.d., 3 μm) with a Synchronis™ HILIC precolumn (10 × 4.6 mm i.d., 3 μm) from Thermo Fisher (Waltham, MA, USA) was used, kept at 20 °*C. mobile* phase A was water containing 5 mM ammonium formate and 0.5 % formic acid and mobile phase B was water/acetonitrile (9:1, *v/v*) with 5 mM ammonium formate and 0.5 % formic acid. The flow rate was 1 mL min⁻¹, and the eluent gradient was as follows: start at 10 % A and increase to 40 % A in 8 min, then decrease to 10 % A in 1 min, and kept to 10 % A for 4 min. The electrospray ionisation (ESI) source settings were gas temperature 330 °C, gas flow 13 L min⁻¹, nebuliser pressure 40 psi and capillary voltage 4000 V. Chromatograms were recorded in the positive ionisation mode, with cell acceleration voltage 7 V, using the dynamic MRM (multiple reaction monitoring) scan mode under the conditions showed in Supplementary Table S2. A calibration standard (0–2.5 mM) of 18 amino acids was prepared in acetonitrile/water (1:4, v/v) and norvaline was used as internal standard.

2.3.2. Quantification of free sugars

The extracts were used for the quantification of free sugars in the same LC-MS/MS instrument described above. The column employed was a LUNA® Omega SUGAR 100 Å (150 × 2.1 mm, particle size 3 μm) from Phenomenex (Torrance, CA, USA) provided with a column guard with the same characteristics and kept at 35 °C. A constant flowrate of 0.5 mL min⁻¹ was used and the eluents were ultrapure water (eluent A) and LC-MS/MS grade acetonitrile (eluent B). The following eluent gradient was applied: 10 % A for 5 min, then increasing to 40 % A in 5 min and kept for 6 min, before decreasing to 10 % A in 4 min. The total run time was 20 min with a 12-min post-run. Detection parameters were set as follows: gas temperature 275 °C, gas flow 12 L min⁻¹, nebuliser pressure 50 psi, capillary voltage 6000 V. Chromatograms were recorded in the negative ionisation mode and MRM settings for every compound are shown in Supplementary Table S2. Calibration standards (0–1 mM) of glucose and fructose were prepared in water/acetonitrile (2:8 *v/v*). Trehalose was used as internal standard.

2.3.3. Quantification of ARP

The malt extracts were diluted 50 times (*v/v*) with ultrapure water, filtered through a 0.2-μm syringe filter and analysed with the LC-MS/MS system described above. A Discovery HS F5–3 (150 × 2.1 mm i.d., 3 μm) column, fitted with a column guard of similar characteristics, from Supelco (St. Louis, MO, USA), was used. The column was kept at 55 °C throughout the analysis. Water with 0.1 % formic acid (A) and acetonitrile with 0.1 % formic acid (B) were used as mobile phases at a constant flowrate of 0.3 mL min⁻¹, following the next gradient: 98 % A for the first 5 min, then decreasing to 0 % A within 3.5 min, then kept for 6 min at 0 % A and increased back to 98 % A within 0.5 min. The total runtime was 15 min with additional 15 min post-run for equilibration. The MS/MS detector was set at the following conditions: gas

temperature 265 °C, gas flow 13 L min⁻¹, nebuliser 40 psi, capillary voltage 4000 V, positive mode, cell accelerator voltage 4 V. MRM settings can be found in Supplementary Table S2. Calibration standards (0–1000 μg/L) were prepared in ultrapure water and no internal standard was used for ARP.

2.4. Quantification of Strecker aldehydes

Ground malt samples (1.0 g for experiments at 65 and 78 °C; 0.5 g for 90 °C) were weighed in 20-mL screw-capped SPME vials, together with 5 mL of saturated NaCl aqueous solution and 5 μL of internal standard solution (100 mg/L of 2-methylpentanal and 100 mg/L of 2-methylbenzaldehyde in absolute ethanol). 2-Methylpentanal was used as internal standard for 2-methylpropanal, 2-methylbutanal, 3-methylbutanal, and methional; and 2-methylbenzaldehyde for phenylacetaldehyde. The samples were incubated at 50 °C for 10 min and then a PDMS/DVB/Carboxen® SPME fibre was exposed to the headspace of the vial for 20 min. The fibre was desorbed into the injection port at 250 °C for 20 min. A 7890 A gas chromatography system was used, coupled to a 5975C mass spectrometry detector from Agilent. The chromatographic separation was achieved with a Zebron™ ZB-5MSi column (30 m, 0.25 mm, 1 μm) from Phenomenex®. The following temperature gradient was used: 50 °C for 2 min, then 6 °C min⁻¹ up to 300 °C and kept at this temperature for 15 min. The single ion mode (SIM) was applied with a dwell time of 250 ms for every ion. The following ions were monitored, the first of them being used for quantification: 41 and 72 for 2-methylpropanal, 41 and 57 for 2-methylbutanal and 3-methylbutanal, 58 and 71 for 2-methylpentanal, 48 and 104 for methional, and 91 and 120 for phenylacetaldehyde and 2-methylbenzaldehyde. The standards for calibration (0–1000 μg/L) were spiked in freeze-dried green malt in order to account for the matrix effects on the release of the volatiles to the headspace of the samples. The analyses were performed in duplicate.

2.5. Kinetic modelling

The kinetic rate constants, k, used in the kinetic model were expressed in the form of the re-parametrised Arrhenius equation:

$$k = k' \bullet e^{\frac{Ea}{Rg}\left(\frac{1}{T_{ref}} - \frac{1}{T}\right)} \tag{1}$$

where T_{ref} is a reference temperature (set at 343.15 K in this study, i.e., 70.00 °C), T is the experimental temperature (K), Ea is the activation energy (J mol⁻¹), Rg is the universal gas constant (8.314 J mol⁻¹ K⁻¹), and k' is the rate constant at T_{ref}. Multi-response parameter estimation and model simulations were performed using the Athena Visual Studio programme (version 14.2) (AthenaVISUAL Inc., Naperville, IL, USA). To account for statistical complications that arise in multiresponse experiments, Bayesian estimation for multiple responses (diagonal covariance) and the determinant criterion were chosen to estimate the parameters k' and Ea (Martins & Van Boekel, 2005a).

For discriminating between models, the sum of squared residuals and the Akaike information criterion (AIC) were employed (Martins & Van Boekel, 2003). AIC was calculated as follows:

$$AIC = nln\left(\frac{SS}{n}\right) + 2(p+1) \tag{2}$$

where *n* is the number of data points, SS is the sum of squared residuals, and *p* is the number of estimated parameters. AIC values were calculated for different models, and the ones with higher AIC discarded. AIC is widely employed for the discrimination between kinetic models, and it takes into account both the accuracy of the models (sum of squared residuals) as well as their complexity (number of parameters).

2.6. Statistical analysis

Two-way ANOVA (multivariate linear analysis) was carried out with SPSS® Statistics Version 22 from IBM® (Armonk, NY, USA).

3. Results and discussion

3.1. Kinetics of precursors, intermediates and Strecker aldehydes

In the present study, the formation of five Strecker aldehydes (3-methylbutanal, 2-methylbutanal, 2-methylpropanal, phenylacetaldehyde and methional) was monitored during the curing stage of kilning of barley malt. The amino acids from which these aldehydes are derived
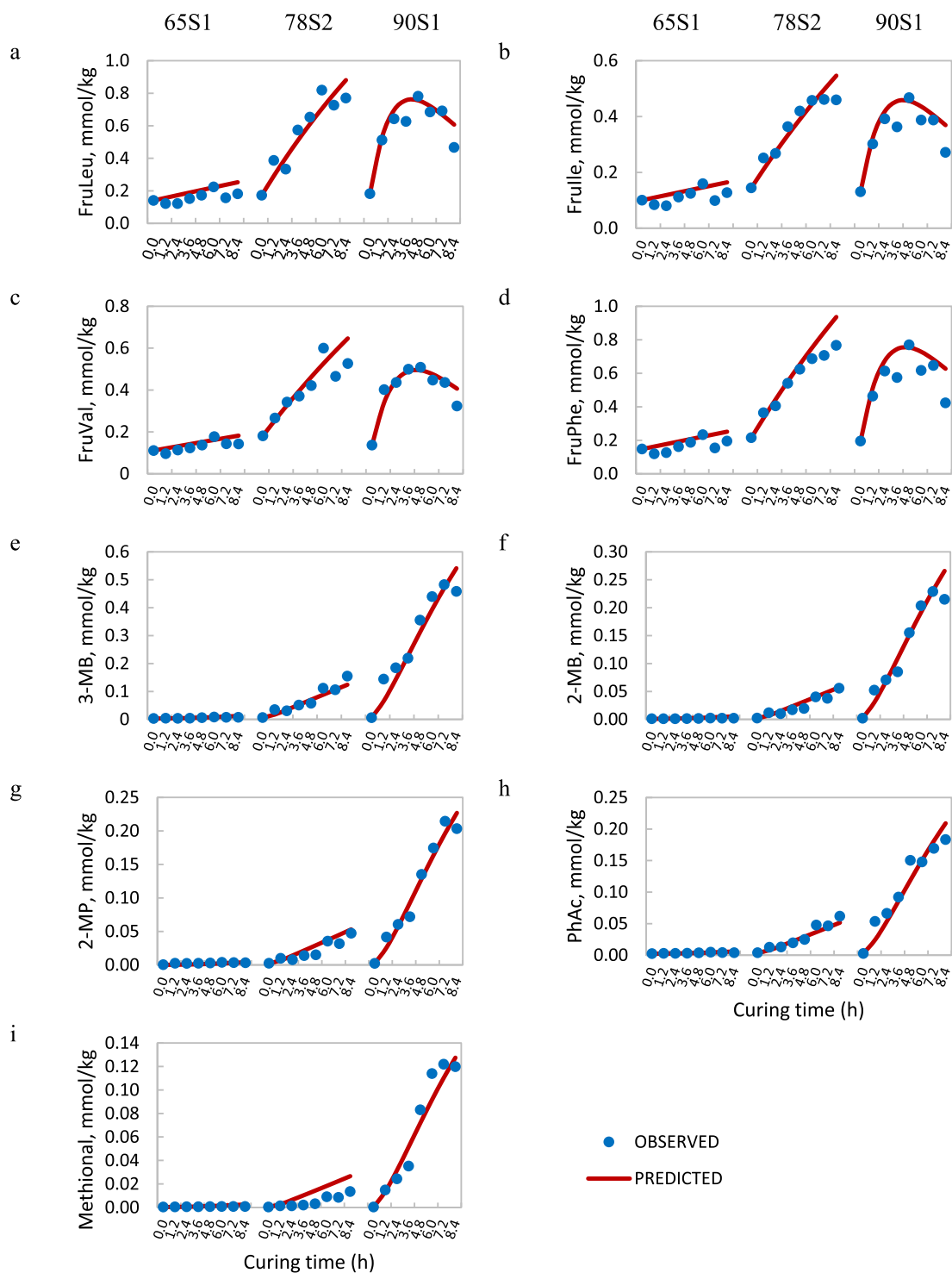

Fig. 1. Concentration of ARP and Strecker aldehydes during the curing stage of kilning Sample coding: curing temperature (65, 78 or 90°C), S for "spring variety", and replicate number (1 or 2). 3-MB: 3-methylbutanal; 2-MB: 2-methylbutanal; 2-MP: 2-methylpropanal; PhAc: phenylacetaldehyde. The whole set of data can be found in Supplementary Fig. S1.

(leucine, isoleucine, valine, phenylalanine and methionine) were quantified too, together with the kinetically important reducing sugars (glucose and fructose) that also participate in the Maillard reaction. Additionally, stable intermediates ARP (glucose-amino acids conjugates) were determined analytically and employed in the kinetic model (FruAla, FruGly, FruIle, FruLeu, FruPhe, FruPro, FruVal). Other amino acids not directly involved in the formation of the target aldehydes were quantified. Fig. 1 shows the concentration of ARP and Strecker aldehydes for a selection of malt samples cured at three different temperatures. The complete data for sugars, amino acids, ARP and Strecker aldehydes for spring and winter barleys in duplicate are shown in Supplementary Fig. S1.

The temperatures used in this research (65, 78 and 90 °C) were chosen in order to cover the normal range of curing temperatures for pale malts (Yahya et al., 2014). The results showed that the formation of Strecker aldehydes was strongly dependent on the curing temperature, with the lowest concentrations found at 65 °C and the highest at 90 °C (Fig. 1 and Supplementary Figs. S1o to S1s). Regarding the differences between varieties, spring barley malt contained higher levels of Strecker aldehydes in malts kilned at 90 °C at the end of the curing stage, but the opposite was observed at 78 °C, with higher averaged amounts for winter barley malts. At 65 °C the difference was minimal. However, the analysis of variance showed no significant difference ($p > 0.05$) between the winter and the spring barleys for any of the aldehydes (Supplementary Table S3).
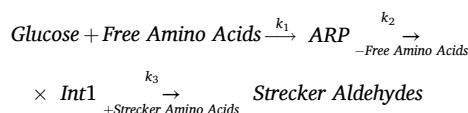
The data from ARP followed a trend typical of a reactive intermediate, increasing in the early stages of the process and then decreasing (Fig. 1 and Supplementary Fig. S1j to S1n). The concentration of aldehydes increased during processing, and in the case of methional only, they levelled off towards the end mainly due to depletion of the precursors. Sugars, however, showed a less clear trend due to a greater scatter of the data (Supplementary Figs. S1h to S1i). In the case of glucose and fructose, the high variability of the results was associated with the fact that the raw materials (i.e., the green malts) used for this study were collected from industrial-scale germination boxes. The heterogeneity of the sample and other less well controlled factors, such as the degree of transformation of the starch into fermentable sugars in the germinating grain, are possible reasons behind the variability of sugars and amino acids. Besides, the green malts were kilned in a micro-malting equipment fitted with eight compartments. The samples were taken randomly from these compartments or boxes, and the different positions in the oven probably contributed to the variability of the results due to a non-homogeneous temperature of the air and flowrates through the boxes. Furthermore, real food matrices often present the disadvantage of having much higher variability in their measured responses than model systems due to unaccountable chemical and/or physical interactions. Despite the variation of sugars and amino acids, the results for ARP and Strecker aldehydes had small variation and distinct trends.

3.2. Development of the kinetic model

The chemistry of the Maillard reaction is complex, with reactions occurring in series and in parallel, the formation of multiple precursors and intermediates of different stability, and a wide variety of products. Furthermore, if the aim is to understand the kinetics of these reactions, the task is even harder. For this purpose, multi-response kinetic modelling was employed in order to solve a system of differential equations derived from a mechanism comprising several kinetic parameters. The kinetic mechanism is structured in such a way as to represent just the rate limiting steps in the chemical reactions under investigation. Multi-response modelling employs all the model responses simultaneously, thus providing a more reliable estimation of the unknown parameters.

The development of the kinetic model was based on previous studies from our research group. Balagiannis et al. (2009) proposed a kinetic model which involved the formation of 3-methylbutanal and 2-methylbutanal in a meat model system heated at 120 °C, 130 °C and 140 °C. Additionally, Parker et al. (2012) and Balagiannis et al. (2019) developed and proposed comprehensive kinetic models on the formation of acrylamide in French fries. Although acrylamide is not a volatile aroma compound, its formation follows a pathway similar to that of the Strecker aldehydes, with the presence of highly reactive dicarbonyl intermediates, and the formation of ARP. Based on the aforementioned studies, a simplified kinetic model was chosen as a starting point for the present study. The process of developing a kinetic model usually involves proposing many variations of a basic mechanism, evaluating the integrity of the estimated parameters and tracking the fit of the model to the analytical data and other quality factors, such as the normality on the distribution of the residuals. The choice of reactions assessed is logically developed based on the underlying chemistry of the Maillard reaction. In our case, a basic reaction backbone was chosen, consisting of the reaction of glucose and an amino acid, resulting in the formation of an ARP, then an intermediate (Int1) with the release of that amino acid, and the further reaction of another amino acid with Int1 to produce a Strecker aldehyde:

$$Glucose + Free\ Amino\ Acids \xrightarrow{k_1} ARP \underset{-Free\ Amino\ Acids}{\xrightarrow{k_2}}$$

$$\times\ Int1 \underset{+Strecker\ Amino\ Acids}{\xrightarrow{k_3}} Strecker\ Aldehydes$$

Among the variations applied to this route, the most significant ones were the addition of a reaction for the formation of Maillard reaction products (MRP) from Int1 and amino acids, and the formation of Int1 from the degradation of fructose. Kato et al. (1969) reported that fructose was converted to a key reactive intermediate (corresponding to Int1, in our study) via a single kinetic step, while in the case of glucose a two-step process was required. This was confirmed by Mundt and Wedzicha (2003) when they studied the kinetics of browning in a glucose (1.0 M)/fructose (1.0 M)/glycine (0.5 M) mixture (pH 5.5, 0.2 M acetate buffer) heated at 55 °C. In addition, the degradation of fructose into a reactive intermediate such as 1-deoxyglucosone, has been reported in a kinetic mechanism for the formation of α-dicarbonyl compounds in a glucose/wheat model systems heated at 160–200 °C (Kocadağlı & Gökmen, 2016). The addition of the one-step degradation of fructose improved the fit of the model in terms of a lower sum of squared residuals. This value was used as a guide to judge the goodness of fit of the models in order to verify whether the model improved or worsened after a modification (AIC was used to discriminate between models in case of ambiguity).

Other modifications to the model did not produce any reductions in the sum of squared residuals, and were hence discarded. One of these was a route for the direct breakdown of the ARP into Strecker aldehydes and a sugar degradation product (SDP), without the intermediate SCDC. This has been proposed by some researchers as a possible mechanism for the formation of Strecker aldehydes from ARP (Cremer et al., 2000; Yaylayan, 2003). This route was tested in a kinetic model, but the sum of the squared residuals was higher than for the model including Int1. The rejection of this model was also based on AIC, which was indeed higher for this model (AIC = 672) than for the one with Int1 (AIC = 639).

Some reactions that were also dismissed were: the degradation of ARP, Int1 or the aldehydes into unknown or non-quantified species, the presence of another intermediate before Int1, or the formation of MRP from amino acids only. These routes either did not produce any relevant improvement of the quality of the model or the parameters related to them were null. The use of individual kinetic rate constants for each reaction has been checked too, but the results showed that the estimated parameters gained in quality (narrower error bars) when they were combined and used in several reactions.
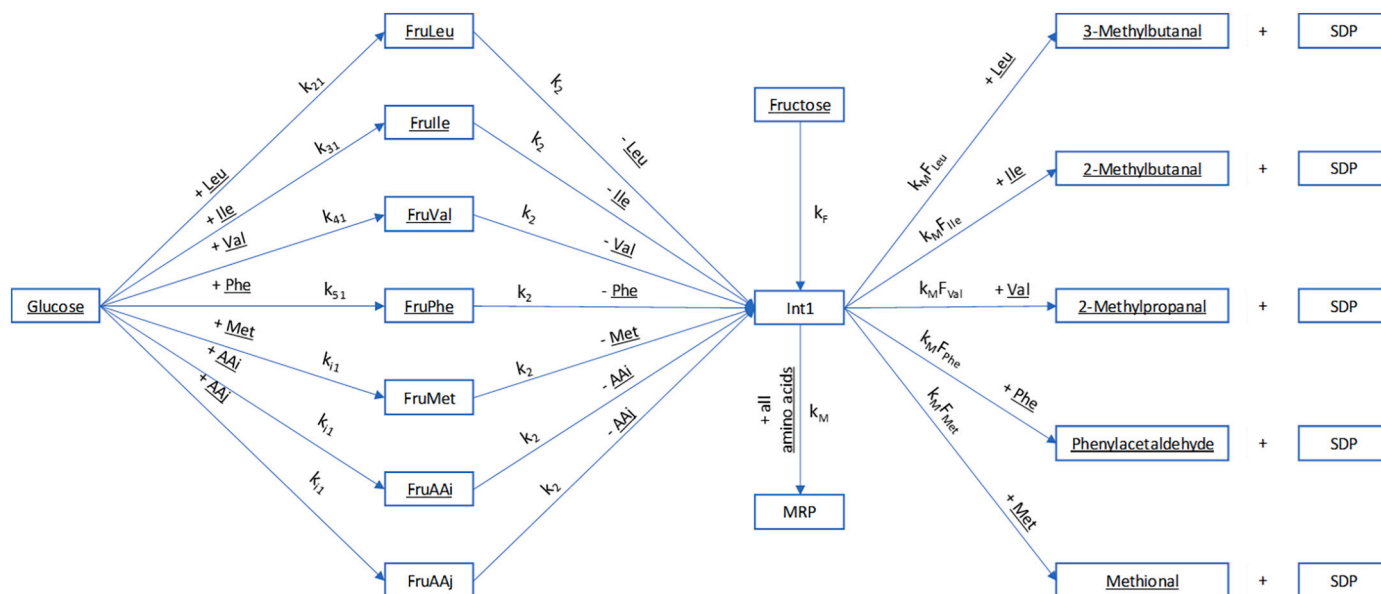
Fig. 2. Postulated kinetic mechanism for the formation of five Strecker aldehydes from glucose, fructose and amino acids. The species underlined were quantified analytically. ki represents the kinetic rate constant involved in each reaction. Fru + Amino acid: Fructosyl derivatives of amino acids (Amadori rearrangement products, ARP); AAi and AAj: pool of amino acids (other than Val, Leu, Ile, Phe and Met) for which their corresponding ARP was quantified analytically or not, respectively; Int1: intermediate products; MRP: Maillard reaction products; SDP: Strecker degradation by-products.

3.3. Postulated kinetic model

After several iterations on various models, we concluded with the kinetic mechanism shown in Fig. 2 for the formation of 2-methylpropanal, 2-methylbutanal, 3-methylbutanal, phenylacetaldehyde and methional via the Maillard reaction combined with the Strecker degradation during the curing stage of malt kilning. According to our kinetic mechanism, glucose reacted with amino acids to form the corresponding N-fructosyl amino acid derivatives (ARPs). Then, the ARPs degraded into a common pool of intermediates (Int1) with concurrent regeneration of the amino acids. The amino acids Val, Leu, Ile, Phe and Met and their corresponding ARP were included in the model as standalone compounds since they were explicitly quantified. FruMet was not quantified instrumentally and for this reason was estimated by the model. The rest of the amino acids was split and their concentrations pooled into two categories: AAi for those whose ARP were quantified (i. e. FruAAi) and AAj for those whose ARP were not quantified (i.e. FruAAj). Thus, AAi was the sum of Ala, Gly and Pro and FruAAi was the

sum of FruAla, FruGly and FruPro. Since FruAAj were not determined analytically, their pooled concentrations were estimated by the model. The amino acids that did not participate directly in the formation of Strecker aldehydes (AAi and AAj) did take part during the first stages of the Maillard reaction by reacting with glucose. Also, these amino acids reacted with Int1 for the formation of other MRP including free glycated amino acids (Hellwig & Henle, 2020) and melanoidins.

The intermediate compounds Int1, according to our model, had very low concentrations in relation to other species in this system, with a maximal predicted level of around 0.17 mmol/kg (Supplementary Fig. S2). At lower temperatures, the degradation rate of Int1 was lower than its formation rate; however, at higher temperatures this relationship was reversed especially at higher reaction times where the concentration of sugars was near depletion. Therefore, our suggestion is that Int1 represents a pool of reactive intermediates that once they are formed, react rapidly to form other compounds. These intermediates were not quantified in this study, but we assumed that they corresponded to a pool of SCDC, such as glyoxal and methylglyoxal. Int1

Table 1
Parameter estimates for the postulated kinetic model shown in Fig. 2.

Parameter	Rate constant function in which the parameter was used	Optimal estimate ± 95 % HPD* (% error)
k'_{21} (kg mmol^{-1} h^{-1})	k_{21}	$1.05 \cdot 10^{-4} \pm 7 \cdot 10^{-6}$ (7 %)
k'_{31} (kg mmol^{-1} h^{-1})	k_{31}	$6.05 \cdot 10^{-5} \pm 4 \cdot 10^{-6}$ (7 %)
k'_{41} (kg mmol^{-1} h^{-1})	k_{41}	$2.57 \cdot 10^{-5} \pm 1 \cdot 10^{-6}$ (6 %)
k'_{51} (kg mmol^{-1} h^{-1})	k_{51}	$5.08 \cdot 10^{-5} \pm 4 \cdot 10^{-6}$ (7 %)
k'_{i1} (kg mmol^{-1} h^{-1})	k_{i1}	$1.16 \cdot 10^{-5} \pm 7 \cdot 10^{-7}$ (6 %)
Ea_1 (kJ mol^{-1})	$k_{21}, k_{31}, k_{41}, k_{51}, k_{i1}$	175 (fixed)
k'_2 (h^{-1})	k_2	$7.30 \cdot 10^{-4} \pm 3 \cdot 10^{-5}$ (5 %)
Ea_2 (kJ mol^{-1})	k_2	315 (fixed)
F_{Leu}		1.000 (upper bound)
F_{Ile}		0.518 ± 0.03 (6 %)
F_{Val}		0.172 ± 0.01 (6 %)
F_{Phe}		0.207 ± 0.01 (5 %)
F_{Met}		0.269 ± 0.02 (9 %)
k'_M (kg mmol^{-1} h^{-1})	k_M	$5.19 \cdot 10^{-4} \pm 5 \cdot 10^{-4}$ (92 %)
Ea_M (kJ mol^{-1})	k_M	255 (fixed)
k'_F (h^{-1})	k_F	$1.82 \cdot 10^{-2} \pm 3 \cdot 10^{-3}$ (18 %)
Ea_F (kJ mol^{-1})	k_F	121 (fixed)

* Highest posterior density
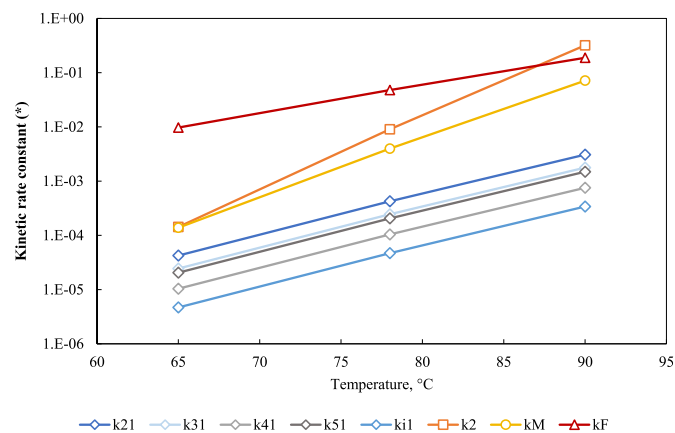
Fig. 3. Effect of temperature on the kinetic rate constants. (*) k_{21}, k_{31}, k_{41}, k_{51}, k_{i1} and k_M in kg mmol^{-1} h^{-1}; k_2 and k_F in h^{-1}.

further reacted with free amino acids leucine, isoleucine, valine, phenylalanine and methionine in order to form the Strecker aldehydes 3- and 2-methylbutanal, 2-methylpropanal, phenylacetaldehyde and methional, respectively. In parallel, Int1 reacted with all the amino acids and formed a group of unidentified Maillard compounds (MRP).

Overall, the kinetic mechanism of Fig. 2 is translated into the following system of differential equations:

$$\frac{d[Gluc]}{dt} = -[Gluc] \cdot (k_{21}[Leu] + k_{31}[Ile] + k_{41}[Val] + k_{51}[Phe] + k_{i1}([Met] + [AAi] + [AAj]))$$

$$\frac{d[Fruc]}{dt} = -k_F[Fruc]$$

$$\frac{d[Leu]}{dt} = -k_{21}[Gluc][Leu] + k_{22}[FruLeu] - k_M[Int1][Leu]$$

$$\frac{d[Ile]}{dt} = -k_{31}[Gluc][Ile] + k_{32}[FruIle] - k_M[Int1][Ile]$$

$$\frac{d[Val]}{dt} = -k_{41}[Gluc][Val] + k_{42}[FruVal] - k_M[Int1][Val]$$

$$\frac{d[Phe]}{dt} = -k_{51}[Gluc][Phe] + k_{52}[FruPhe] - k_M[Int1][Phe]$$

$$\frac{d[Met]}{dt} = -k_{i1}[Gluc][Met] + k_{i2}[FruMet] - k_M[Int1][Met]$$

$$\frac{d[AAi]}{dt} = -k_{i1}[Gluc][AAi] + k_{i2}[FruAAi] - k_M[Int1][AAi]$$

$$\frac{d[AAj]}{dt} = -k_{i1}[Gluc][AAj] + k_{i2}[FruAAj] - k_M[Int1][AAj]$$

$$\frac{d[FruLeu]}{dt} = k_{21}[Gluc][Leu] - k_{22}[FruLeu]$$

$$\frac{d[FruIle]}{dt} = k_{31}[Gluc][Ile] - k_{32}[FruIle]$$

$$\frac{d[FruVal]}{dt} = k_{41}[Gluc][Val] - k_{42}[FruVal]$$

$$\frac{d[FruPhe]}{dt} = k_{51}[Gluc][Phe] - k_{52}[FruPhe]$$

$$\frac{d[FruMet]}{dt} = k_{i1}[Gluc][Met] - k_{i2}[FruMet]$$

$$\frac{d[FruAAi]}{dt} = k_{i1}[Gluc][AAi] - k_{i2}[FruAAi]$$

$$\frac{d[FruAAj]}{dt} = k_{i1}[Gluc][AAj] - k_{i2}[FruAAj]$$

$$\begin{aligned}\frac{d[Int1]}{dt} = &\ k_F[Fruc] + k_{22}[FruLeu] + k_{32}[FruIle] + k_{42}[FruVal] \\ &+ k_{52}[FruPhe] + k_{i2} \cdot ([FruMet] + [FruAAi] + [FruAAj]) \\ &- k_M[Int1] \cdot ([Leu] + [Ile] + [Val] + [Phe] + [Met] + [AAi] \\ &+ [AAj])\end{aligned}$$

$$\frac{d[3MB]}{dt} = k_M F_{Leu}[Int1][Leu]$$

$$\frac{d[2MB]}{dt} = k_M F_{Ile}[Int1][Ile]$$

$$\frac{d[2MP]}{dt} = k_M F_{Val}[Int1][Val]$$

$$\frac{d[PhAc]}{dt} = k_M F_{Phe}[Int1][Phe]$$

$$\frac{d[Meth]}{dt} = k_M F_{Met}[Int1][Met]$$

$$\begin{aligned}\frac{d[MRP]}{dt} = &\ k_M[Int1] \cdot \{(1 - F_{Leu})[Leu] + (1 - F_{Ile})[Ile] + (1 - F_{Val})[Val] + (1 \\ &- F_{Phe})[Phe] + (1 - F_{Met})[Met] + [AAi] + [AAj]\}\end{aligned}$$

$$\begin{aligned}\frac{d[SDP]}{dt} = &\ k_M[Int1] \cdot (F_{Leu}[Leu] + F_{Ile}[Ile] + F_{Val}[Val] + F_{Phe}[Phe] \\ &+ F_{Met}[Met])\end{aligned}$$

Some of the reactions in the kinetic model (Fig. 2) shared the same kinetic rate constant. Reducing the number of parameters was found to improve the quality of the parameter estimates by lowering the confidence interval without reducing the overall fit of the model. Individual kinetic rate constants were used for the reaction between glucose and Leu, Ile, Val and Phe (k_{21}, k_{31}, k_{41}, k_{51}, respectively), whereas a common k_{i1} was used for Met, AAj and AAi. For all ARP, the kinetic rate constants for the degradation reaction were the same (k_2), all depending on the same parameters k'$_2$ and Ea$_2$. Besides, k_M was used for all reactions between Int1 and the amino acids. In the case of the amino acids forming Strecker aldehydes, k_M was multiplied by a factor F$_{amino\ acid}$ which represented the proportion of each amino acid that was used to form the aldehyde; the rest (1-F$_{amino\ acid}$) followed the route for the formation of MRP. For example, F$_{Leu}$ represented the proportion of reacted Leu that was used in the formation of 3-methylbutanal, while 1-F$_{Leu}$ was used to form MRP. For some samples, a decrease on the concentration of Strecker aldehydes at the end of the curing step at 90 °C was observed. These losses of these volatile compounds might be due to evaporation
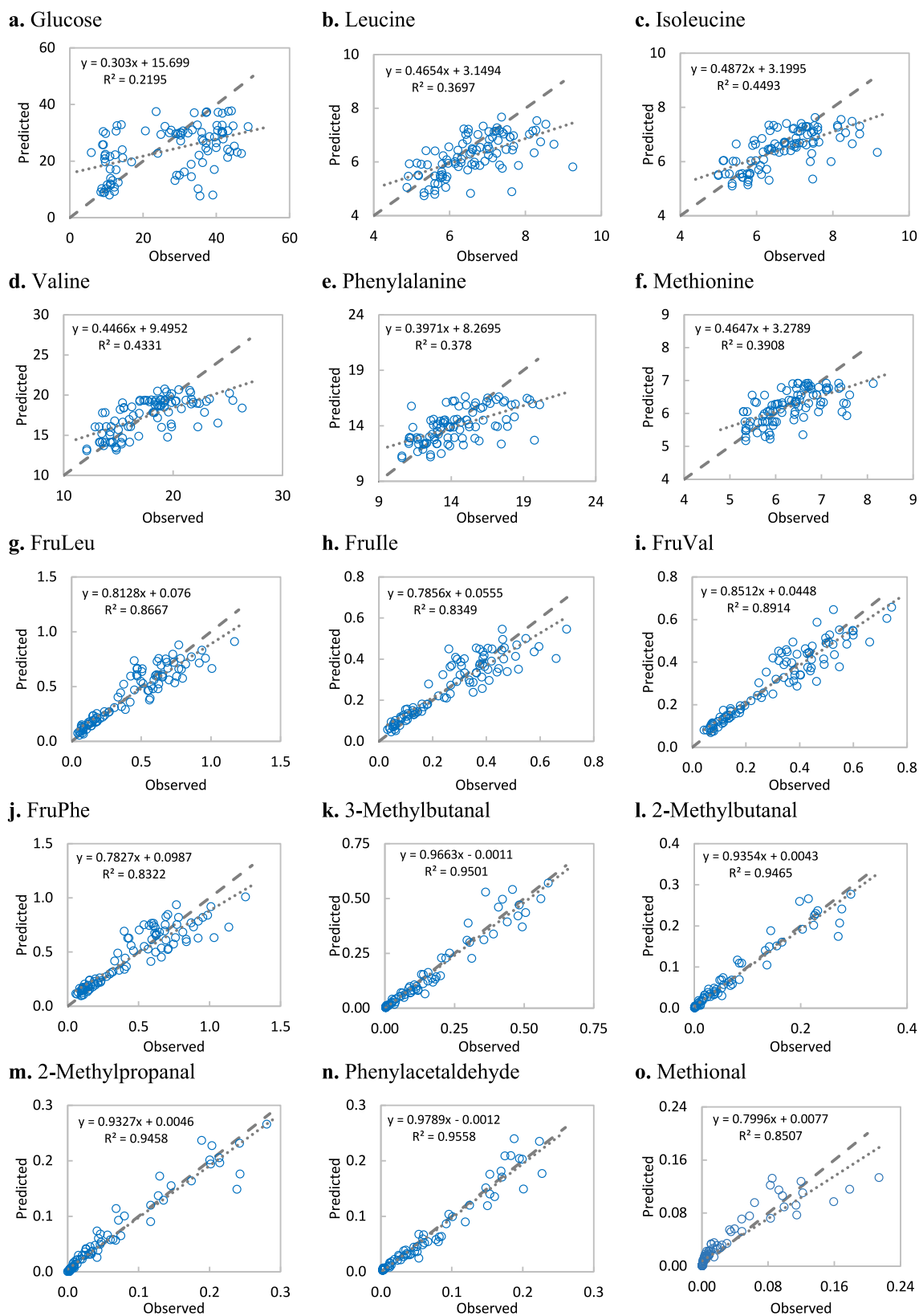
Fig. 4. Predicted against observed values (all in mmol/kg) from the kinetic model. Dashed lines correspond to the line of perfect fit (predicted = observed); dotted lines represent the actual linear fit (equations and regression coefficients R^2 shown in every graph).
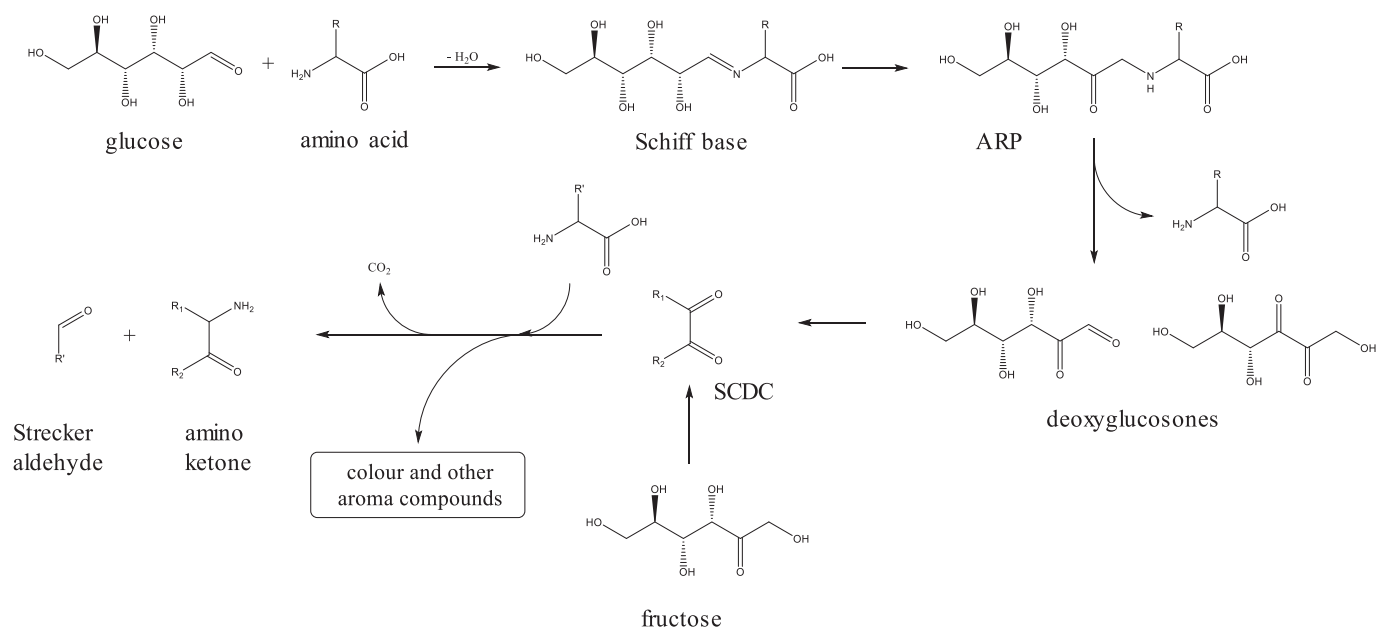
Fig. 5. Postulated chemical mechanism for the formation of Strecker aldehydes within the Maillard reaction from glucose and fructose and amino acids. ARP: Amadori rearrangement product, SCDC: short chain dicarbonyls.

and/or thermal degradation into other compounds and were only between the last two sampling timepoints. Trying to fit this particular behaviour by adding a degradation reaction to the system would have led to overfitting of the model.

The parameters k' and Ea were optimised by Bayesian estimation for multiple responses in order to minimise the sum of squared residuals of the predicted vs. observed values. The Bayesian approach combines prior knowledge about the parameters and the information from the data and in order to provide more accurate and realistic estimates (Van Boekel, 2020). The estimation was performed in several runs, alternatively keeping one group of parameters fixed (k' or Ea) and estimating the rest. The optimisation was achieved with the determinant criterion (Box & Draper, 1965) which is ideal for multi-response calculations since it avoids some statistical restraints/implications that need to be addressed in the usual least square minimisation (i.e. normality of residuals and error independence for each response) (Balagiannis, 2015). The residual plots (not shown) were checked, and they were randomly scattered, which is an extra indication of the good quality of the model. Table 1 shows the optimal values for the estimated parameters. The quality of most of the parameters estimated was very good based on their confidence intervals (highest posterior density, HPD, for Bayesian statistics), these being ≤ 10 % of the actual estimated value for 10 out of 13 parameters. Two parameters, k'_F and k'_M, showed greater errors of 18 and 92 %, respectively. The high uncertainty of k'_M was due to the fact that it was associated with the degradation of Int1 whose concentration was not determined analytically. F_{Leu} reached the upper limit for the F factors, i.e., 1.0. This meant that 100 % of leucine that reacted with Int1 was used to generate 3-methylbutanal, and not MRP. For the formation of 2-methylbutanal, F_{Ile} was 51.8 %, whereas lower values (around 20 %) were estimated for 2-methylpropanal, phenylacetaldehyde and methional (Table 1).

The activation energies, Ea, were kept fixed at the last calculation run in order to reduce the system's HPD intervals, hence no confidence intervals are reported for them. Activation energies were found to be in the range between 121 and 315 kJ mol^{-1} (Table 1), generally higher than similar kinetic studies. In our study, the activation energy related to the formation of Strecker aldehydes, EaM, was 255 kJ mol^{-1}, but Ea2, for the cleavage of ARP, was even higher (315 kJ mol^{-1}). Huang et al. (2016) studied the formation of 2- and 3-methylbutanal using maltose or

glucose as reducing sugars in a wort-like model system. They reported activation energies in the range of 83–121 kJ mol^{-1}, depending on the amino acid and sugar. Balagiannis et al. (2009) reported an activation energy of 48.7 kJ mol^{-1} for the formation of these two aldehydes in a heated extract of beef liver. Higher values were found for the formation of acetaldehyde, 2-methylpropanal, 2-methylbutanal and 3-methylbutanal in a low moisture model system, between 115 and 124 kJ mol^{-1} (Cremer & Eichner, 2000). Other authors reported higher Ea (237 kJ mol^{-1}) for the degradation of glucose into formic and acetic acids (Martins & Van Boekel, 2005b).

Ea values determine how sensitive the kinetic rate constants are to temperature changes. Fig. 3 shows the effect of temperature on the kinetic rate constants employed in our model where the slope of the lines depends on the respective activation energies. Higher activation energies lead to steeper slopes, where a temperature rise brings about larger increases in kinetic rate constants. In that sense, since the intermediate steps (k_2, k_M) showed higher Eas than the first steps (k_1, k_F), and as processing temperature increased, the degradation rate of the intermediate compounds increased to a larger extent than that of the precursors. Therefore, for the same amount of degraded initial precursors, a higher amount of Strecker aldehydes was formed in relation to lower temperatures. Consequently, by keeping the curing temperature low, the formation of Strecker aldehydes was considerably suppressed, as it was also evident from our results (Supplementary Fig. S1). Overall, by employing lower temperatures during malt kilning, the reduction of the formation of Strecker aldehydes is achieved not only because at lower temperatures the rate constants of the reaction are lower in general, but also due to the considerable reduction of k_2' in relation to the other reaction rate constants since Ea2 has the highest value.

Overall, the quality of the fit of the model was good, which is remarkable considering the complexity that is involved in the study of an authentic commodity which was processed under industrial-like conditions. For the reasons explained in Section 3.1, sugars and amino acids had the least good fit. Predicted vs. observed data (Fig. 4) showed R^2 close to or higher than 0.80 for ARP and around 0.95 for all Strecker aldehydes apart from methional (0.81). Besides, the slopes were close to 1 for these compounds (dotted lines in the graphs), showing that the predicted data matched closely the observed.

3.4. Discussion of the chemical mechanism

The kinetic model was built upon the known chemistry of the Maillard reaction and the Strecker degradation. In conjunction with the experimental results, we postulate the kinetic mechanism in Fig. 5 for the formation of Strecker aldehydes. As described by Hodge (1953), reducing sugars react with amino acids to form ARP via the formation of a Schiff base. Several ARP have already been identified in barley malt (Meitinger et al., 2014) and different types of beer (Hellwig et al., 2016). Then, the amino acid fragment of the ARP is regenerated, and the sugar backbone forms a vicinal dicarbonyl, such as 3-deoxyglucosone from glucose. This compound has been already identified in barley malt and formed during malt kilning (Nobis et al., 2019). Martins and Van Boekel (2005a) identified and monitored the formation of 1- and 3-deoxyglucosone from the reaction between glucose and glycine at high temperature (80–120 °C). These dicarbonyls, in turn, break down further into a pool of reactive SCDC, such as glyoxal, methylglyoxal, 2,3-butanedione, and others (Kocadağlı & Gökmen, 2016). These reactive compounds, SCDC, further react with amino acids, and following a cascade of reactions the carboxyl group of the amino acid part is released as CO_2 generating the Strecker aldehyde, whereas the SCDC part forms an amino ketone (Parker, 2015). In our kinetic model, these amino ketones can be identified as SDP (Strecker degradation by-products), which also covered any other products that derive from these compounds.

Kinetic models comprise rate limiting reactions which represent a simplification of the real chemical mechanism. In most cases, the presence of unstable species is translated into fast reactions from a kinetic point of view. These species are formed and quickly degrade to other compounds; thus, although these reactions are considered for chemical mechanisms, in kinetic models they are omitted. Huang et al. (2016) postulated a kinetic model for the formation of 2- and 3-methylbutanal from reducing sugars and isoleucine and leucine, respectively. The proposed model consisted of three reactions in series, with no parallel reactions. The formation of these aldehydes in a meat extract was explained by a kinetic model where Strecker amino acids react with a cluster of very reactive intermediates from the degradation of glucose (Balagiannis et al., 2009). Moreover, kinetic mechanisms with a similar rational and structure have been used successfully for modelling the formation of acrylamide in foods. Acrylamide is formed from the reaction of asparagine with reducing sugars or Maillard derived reactive intermediates, such as dicarbonyls (Balagiannis et al., 2019).

4. Conclusions

The formation of five Strecker aldehydes (2-methylpropanal, 2- and 3-methybutanal, phenylacetaldehyde and methional) during kilning of commercial malt at pilot scale has been studied. The results demonstrated the clear dependence of the concentration of Strecker aldehydes in malt with the temperature of the curing stage of kilning. The highest concentrations of these compounds were reached at 90 °C. Multiresponse modelling has been used as a tool to construct a mechanistic kinetic model in which the most important rate limiting reactions have been identified. This mathematical model is based on the known chemistry of the Maillard reaction and Strecker degradation. After having estimated the kinetic parameters of the model, the effect of temperature and time on the formation of Strecker aldehydes was quantitatively elucidated, potentially allowing its use for predictive purposes. The estimation of the activation energies indicated that with respect to the kinetic pathways that comprised the model, lower temperatures restrain the degradation of the Amadori products in particular, hence suppressing the formation of Strecker aldehydes.

This model can be used to control and predict the final amount of these important aroma compounds in malt knowing the precursor profile of the different batches of grain and processed under different conditions, and consequently the organoleptic quality of the malt and the beers brewed from them. Although the sensory characteristics of the malts produced have not been studied, we acknowledge that it is of great importance to the brewing sector and that it should be addressed in future studies. Strecker aldehydes are also key aroma compounds in alcohol-free beers brewed by cold contact fermentation, as well as precursors of the formation of fruity alcohols and esters in alcoholic beers. For the first time, our new model provides the malting industry with the potential to adapt kilning times and temperatures on the basis of the composition of the raw material and thereby achieve consistently high-quality end products.

CRediT authorship contribution statement

José A. Piornos: Writing – review & editing, Writing – original draft, Software, Formal analysis, Data curation, Conceptualization. **Dimitris P. Balagiannis:** Writing – review & editing, Supervision, Software, Funding acquisition, Conceptualization. **Elisabeth Koussissi:** Writing – review & editing, Supervision, Funding acquisition, Conceptualization. **August Bekkers:** Writing – review & editing, Conceptualization. **Johan Vissenaekens:** Writing – review & editing, Conceptualization. **Eric Brouwer:** Writing – review & editing, Supervision, Funding acquisition, Conceptualization. **Jane K. Parker:** Writing – review & editing, Supervision, Project administration, Funding acquisition, Conceptualization.

Declaration of competing interest

The authors declare the following financial interests/personal relationships which may be considered as potential competing interests: José A. Piornos reports financial support, equipment and supplies were provided by Heineken Supply Chain BV. José A. Piornos reports equipment and supplies were provided by Mouterij Albert. Elisabeth Koussissi reports a relationship with Heineken Supply Chain BV that includes: employment. August Bekkers reports a relationship with Heineken Supply Chain BV that includes: employment. Eric Brouwer reports a relationship with Heineken Supply Chain BV that includes: employment. Johan Vissenaekens reports a relationship with Mouterij Albert that includes: employment. If there are other authors, they declare that they have no known competing financial interests or personal relationships that could have appeared to influence the work reported in this paper.

Data availability

Data will be made available on request.

Appendix A. Supplementary data

Supplementary data to this article can be found online at https://doi.org/10.1016/j.foodchem.2024.141532.

References

Akar, T., Avci, M., & Dusunceli, F. (2004). BARLEY post-harvest operations. http://www.fao.org/fileadmin/user_upload/inpho/docs/Post_Harvest_Compendium_-_BARLEY.pdf.

Balagiannis, D. P. (2015). Predicting aroma formation with kinetic models. In J. K. Parker, J. S. Elmore, & L. Methven (Eds.), *Flavour development, analysis and perception in food and beverages* (pp. 211–233). Elsevier Ltd.. https://doi.org/10.1016/b978-1-78242-103-0.00010-2

Balagiannis, D. P., Mottram, D. S., Higley, J., Smith, G., Wedzicha, B. L., & Parker, J. K. (2019). Kinetic modelling of acrylamide formation during the finish-frying of french fries with variable maltose content. *Food Chemistry, 284*, 236–244. https://doi.org/10.1016/j.foodchem.2019.01.075

Balagiannis, D. P., Parker, J. K., Pyle, D. L., Desforges, N., Wedzicha, B. L., & Mottram, D. S. (2009). Kinetic modeling of the generation of 2- and 3-methylbutanal in a heated extract of beef liver. *Journal of Agricultural and Food Chemistry, 57*(21), 9916–9922. https://doi.org/10.1021/jf901443m

Beal, A. D., & Mottram, D. S. (1994). Compounds contributing to the characteristic aroma of malted barley. *Journal of Agricultural and Food Chemistry, 42*(12), 2880–2884. https://doi.org/10.1021/jf00048a043

Box, G. E. P., & Draper, N. R. (1965). The Bayesian estimation of common parameters from several responses. *Biometrika, 52*(3/4), 355–365. https://doi.org/10.2307/2333689

Cremer, D. R., & Eichner, K. (2000). The reaction kinetics for the formation of Strecker aldehydes in low moisture model systems and in plant powders. *Food Chemistry, 71*(1), 37–43. https://doi.org/10.1016/S0308-8146(00)00122-9

Cremer, D. R., Vollenbroeker, M., & Eichner, K. (2000). Investigation of the formation of Strecker aldehydes from the reaction of Amadori rearrangement products with α-amino acids in low moisture model systems. *European Food Research and Technology, 211*(6), 400–403. https://doi.org/10.1007/s002170000196

Gu, Z., Jin, Z., Schwarz, P., Rao, J., & Chen, B. (2022). Uncovering aroma boundary compositions of barley malts by untargeted and targeted flavoromics with HS-SPME-GC-MS/olfactometry. *Food Chemistry, 394*, Article 133541. https://doi.org/10.1016/j.foodchem.2022.133541

Gupta, M., Abu-Ghannam, N., & Gallaghar, E. (2010). Barley for brewing: Characteristic changes during malting, brewing and applications of its by-products. *Comprehensive Reviews in Food Science and Food Safety, 9*(3), 318–328. https://doi.org/10.1111/j.1541-4337.2010.00112.x

Hellwig, M., Witte, S., & Henle, T. (2016). Free and protein-bound Maillard reaction products in beer: Method development and a survey of different beer types. *Journal of Agricultural and Food Chemistry, 64*(38), 7234–7243. https://doi.org/10.1021/acs.jafc.6b02649

Hodge, J. E. (1953). Dehydrated foods. Chemistry of Browning reactions in model systems. *Journal of Agricultural and Food Chemistry, 1*(15), 928–943. https://doi.org/10.1021/jf60015a004

Huang, S., Yu, J., Yin, H., Lu, J., Dong, J., Li, X., Hu, S., & Liu, J. (2016). Optimization of kilning progress for equilibrating multiple parameters that strictly affect malt flavour and sensory evaluation. *Journal of the Institute of Brewing, 122*(4), 706–713. https://doi.org/10.1002/jib.369

Huang, Y., Tippmann, J., & Becker, T. (2016). A kinetic study on the formation of 2- and 3-Methylbutanal. *Journal of Food Process Engineering, 40*(2), 1–11. https://doi.org/10.1111/jfpe.12375

Kato, H., Yamamoto, M., & Fujimaki, M. (1969). Mechanisms of browning degradation of D-fructose in special comparison with D-glucose-glycine reaction. *Agricultural and Biological Chemistry, 33*(6), 939–948.

Kocadağlı, T., & Gökmen, V. (2016). Effects of sodium chloride, potassium chloride, and calcium chloride on the formation of α-Dicarbonyl compounds and furfurals and the development of Browning in cookies during baking. *Journal of Agricultural and Food Chemistry, 64*, 7838–7848. https://doi.org/10.1021/acs.jafc.6b03870

Martins, S. I. F. S., & Van Boekel, M. A. J. S. (2003). Kinetic modelling of Amadori N-(1-deoxy-D-fructos-1-yl)-glycine degradation pathways. Part II - kinetic analysis. *Carbohydrate Research, 338*(16), 1665–1678. https://doi.org/10.1016/S0008-6215(03)00174-5

Martins, S. I. F. S., & Van Boekel, M. A. J. S. (2005a). A kinetic model for the glucose/glycine Maillard reaction pathways. *Food Chemistry, 90*(1–2), 257–269. https://doi.org/10.1016/j.foodchem.2004.04.006

Martins, S. I. F. S., & Van Boekel, M. A. J. S. (2005b). Kinetics of the glucose/glycine Maillard reaction pathways: Influences of pH and reactant initial concentrations. *Food Chemistry, 92*(3), 437–448. https://doi.org/10.1016/j.foodchem.2004.08.013

Meitinger, M., Hartmann, M., & Schieberle, P. (2014). Development of stable isotope dilution assays for the quantitation of Amadori compounds in foods. *Journal of Agricultural and Food Chemistry, 62*(22), 5020–5027. https://doi.org/10.1021/jf501464g

Mundt, S., & Wedzicha, B. L. (2003). A kinetic model for the glucose−fructose−Glycine Browning reaction. *Journal of Agricultural and Food Chemistry, 51*, 3651–3655. https://doi.org/10.1021/jf026027e

Nobis, A., Röhrig, A., Hellwig, M., Henle, T., Becker, T., & Gastl, M. (2019). Formation of 3-deoxyglucosone in the malting process. *Food Chemistry, 290*, 187–195. https://doi.org/10.1016/j.foodchem.2019.03.144

Parker, J. K. (2015). Thermal generation of aroma. In J. K. Parker, J. S. Elmore, & L. Methven (Eds.), *Flavour development, analysis and perception in food and beverages* (pp. 151–185). Elsevier Ltd.. https://doi.org/10.1016/b978-1-78242-103-0.00008-4

Parker, J. K., Balagiannis, D. P., Higley, J., Smith, G., Wedzicha, B. L., & Mottram, D. S. (2012). Kinetic model for the formation of acrylamide during the finish-frying of commercial French fries. *Journal of Agricultural and Food Chemistry, 60*(36), 9321–9331. https://doi.org/10.1021/jf302415n

Perpète, P., & Collin, S. (2000). How to improve the enzymatic worty favour reduction in a cold contact fermentation. *Food Chemistry, 70*, 457–462. https://doi.org/10.1016/S0308-8146(00)00111-4

Piornos, J. A., Balagiannis, D. P., Methven, L., Koussissi, E., Brouwer, E., & Parker, J. K. (2020). Elucidating the odor-active aroma compounds in alcohol-free beer and their contribution to the worty flavor. *Journal of Agricultural and Food Chemistry, 68*(37), 10088–10096. https://doi.org/10.1021/acs.jafc.0c03902

Rizzi, G. P. (2008). The Strecker degradation of amino acids: Newer avenues for flavor formation. *Food Reviews International, 24*(4), 416–435. https://doi.org/10.1080/87559120802306058

Smuda, M., & Glomb, M. A. (2013). Fragmentation pathways during Maillard-induced carbohydrate degradation. *Journal of Agricultural and Food Chemistry, 61*, 10198–10208. https://doi.org/10.1021/jf305117s

Steiner, E., Gastl, M., & Becker, T. (2011). Protein changes during malting and brewing with focus on haze and foam formation: A review. *European Food Research and Technology, 232*(2), 191–204. https://doi.org/10.1007/s00217-010-1412-6

US Foreign Agricultural Service. (2024). Production – Barley. Retrieved from https://fas.usda.gov/data/production/commodity/0430000 Accessed on 10th September 2024.

Van Boekel, M. A. J. S. (2020). On the pros and cons of Bayesian kinetic modeling in food science. *Trends in Food Science and Technology, 99*(2019), 181–193. https://doi.org/10.1016/j.tifs.2020.02.027

Yahya, H., Linforth, R. S. T., & Cook, D. J. (2014). Flavour generation during commercial barley and malt roasting operations: A time course study. *Food Chemistry, 145*, 378–387. https://doi.org/10.1016/j.foodchem.2013.08.046

Yaylayan, V. A. (2003). Recent advances in the chemistry of Strecker degradation and Amadori rearrangement: Implications to aroma and color formation. *Food Science and Technology Research, 9*(1), 1–6. https://doi.org/10.3136/nskkk.50.372

Zhang, N., & Jones, B. L. (1995). Characterization of germinated barley Endoproteolytic enzymes by two-dimensional gel Electrophoresls. *Journal of Cereal Science, 21*(2), 145–153.